A preclinical ultrasound method for assessment of vascular disease progression in murine models.

Abstract

Introduction: Early detection of vascular alterations associated with disease can play a key role in diagnosis and evaluation of treatment strategies. Ultrasound is commonly used for real-time assessment of human blood vessels but the efficacy of preclinical ultrasound at providing a quantitative assessment of mouse models of vascular disease is relatively unknown. In this study, preclinical ultrasound was used in combination with a semi-automatic image processing method to track arterial distension alterations in mouse models of abdominal aortic aneurysm (AAA) and atherosclerosis.

Methods: Longitudinal B-mode ultrasound images of the abdominal aorta were acquired using a preclinical ultrasound scanner. Arterial distension was assessed using a semi-automatic image processing algorithm to track vessel wall motion over the cardiac cycle and a standard, manual analysis method was applied for comparison.

Results: Mean arterial distension was significantly lower in AAA mice between day 0 and day 7 post-onset of disease (p<0.01) and between day 0 and day 14 (p<0.001), while no difference was observed in sham control mice. The manual method detected a significant decrease (p<0.05) between day 0 and day 14 only. Atherosclerotic mice showed alterations in arterial distension relating to genetic

modification and diet. Arterial distension was significantly lower (p<0.05) in Ldlr$^{-/-}$ (++/--) mice fed high fat western diet when compared with both wild type (++/++) mice and Ldlr$^{-/-}$ (++/--) mice fed chow diet. The manual method did not detect a significant difference between these groups.

Conclusions: Arterial distension can be used as an early marker for the detection of arterial disease in small animal models. The semi-automatic analysis method provided increased sensitivity to differences between experimental groups when compared to the manual analysis method. Furthermore, a retrospective power calculation revealed that use of the semi-automatic method reduces the number of animals required per experiment.

Introduction

Ultrasound imaging is routinely used for diagnosis and monitoring of a wide range of diseases.[1] Among these are complex disorders like atherosclerosis and abdominal aorta aneurysm (AAA).[2, 3] These relatively common and potentially life-threatening vascular diseases are often associated with biomechanical changes in the arterial wall.[4, 5] Ultrasound can provide fast, real-time information on the ability of arteries to expand and contract with cardiac pulsation and relaxation, often referred to as arterial distension. A decrease in arterial distension infers increased artery wall stiffness and can serve as an early marker for vascular changes associated with cardiovascular disease.[6, 7] B-mode ultrasound has been related to traditional as well as new risk factors [8] and is commonly used to assess vessel plaque burden and morphological parameters such as lumen diameter and intimal-

medial thickness (IMT).[7] However, current ultrasound methods for investigation of arterial disease are often deemed less reproducible and more imprecise than another imaging modalities such as computed tomography (CT) and angiography.[9, 10] Often only changes that occur late in the disease process can be detected, limiting time for preventative treatment.[7] It is known that functional alternation of the arterial wall occurs in the early stages of vascular disease, before any structural changes become visible[11] and arterial distension may be an important marker for early detection of vessel abnormalities.[12, 13]

Preclinical imaging studies have the potential to enhance our understanding of such diseases and can influence the development of new imaging techniques and therapeutic strategies that can be applied in clinical practice.[14, 15] Mouse models of disease are often used for studying human disease processes, and so far they remain the best available models of abdominal aortic aneurysm (AAA) and atherosclerosis.[16] There are several chemically-induced AAA models used that differ in mechanism of aneurysm induction and deterioration of aortic walls such as calcium chloride ($CaCl_2$), angiotensin II (AngII) and the porcine pancreatic elastin model.[16, 17] The most commonly used model requires subcutaneous infusion of angiotensin II (AngII) into apolipoprotein E-deficient (ApoE$^{-/-}$) mice via an implanted osmotic pump. [18] ApoE $^{-/-}$ and low-density lipoprotein receptor deficient (Ldlr $^{-/-}$) mice are also the two common strains used in studies of atherosclerosis.[16, 19] The mechanism of developing atherosclerotic lesions in these two strains differs. The Apoe$^{-/-}$ mice develop spontaneous lesions as they age and these can be aggravated

by feeding mice with high fat (Western) diet, while Ldlr [-/-] mice can develop atherosclerosis only in the presence of fatty diet.[16]

Previous approaches for quantification of AAA or atherosclerotic lesions often required sacrifice of mice for ex-vivo or sectioned tissue analysis.[20, 21] Recent advances in high-frequency preclinical ultrasound with its increased spatial resolution and short image acquisition times have enabled non-invasive monitoring and quantification of disease progression.[22] A number of in-vivo imaging studies have been carried out on mice demonstrating a correlation between high-frequency ultrasound and standard ex-vivo methods.[23-27] However, many of the current preclinical ultrasound-based methods in use (for example: assessment of morphology, circumferential strain, dimensions and wall stiffness) suffer from drawbacks including high user-dependency of the method with regard to acquisition mode, measurement (e.g. diameter), image angle (long or short axis) and analysis methods applied.[28, 29] These factors ultimately lead to high variability of the physiological parameters under study.[30]

Since there is currently no gold standard analysis method, we applied a technique developed by Kanber and Ramnarine that uses a probabilistic approach for dynamically measuring the vessel lumen diameter.[31] The method was applied to high-resolution preclinical ultrasound images of the abdominal aorta in two murine models of arterial disease (AAA and atherosclerosis) and was compared to the standard analysis method of manually measuring vessel diameter at systole and diastole. To further confirm the feasibility of the semi-automatic method, ultrasound data were validated with histological tissue staining. We demonstrate

that this novel analysis method has the advantage of reduced user-dependency, and improved reproducibility and sensitivity. We also confirm the hypothesis that arterial distension can be used as an early marker for detection of vascular disease.

Materials and Methods

Animals

All work was conducted in accordance with the British Home Office Regulations (Animal Scientific Procedures Act 1986; Project licences 70/8740 and 40/4332) and following institutional ethical approval. Mice were obtained from Charles River UK Ltd (Kent, UK) and were subsequently maintained at the University of Leicester. Experiments are reported in accordance with the Animal research reporting of *in vivo* experiments (ARRIVE) guidelines. Mice were housed in a specific pathogen free (SPF) facility, in groups in individually ventilated cages with negative air pressure and kept in a room with a 12-hour light/dark cycle and a temperature of 22°C. Mice were allowed free access to standard rodent chow (TestDiet, 5LF2) and water. All cages contained bedding, wood shavings, and a cardboard tube for environmental enrichment.

Disease Models

Study 1 – AAA model. Eleven two-month old B6.129P2-ApoEtm1unc/J (ApoE– knockout) male mice weighing between 24 and 25.7g were included in the study. Alzet osmotic mini-pumps (Alzet® 2004, Durect™; CA, USA) were implanted

subcutaneously under isoflurane (5% for induction, 1-2% for maintenance) inhalant anesthesia mixed with oxygen. The mice were infused for 28 days with either normal saline for the sham control group (n=5) or AngII (1000ng/kg/min) for the AAA group (n=6). Mice were monitored closely after surgery for any signs of distress, dehydration or weight loss.

The abdominal aorta of each mouse was scanned once per week using a preclinical ultrasound scanner (refer to Ultrasound imaging section below). All mice were scanned before surgery at day zero (baseline) and one week after surgery, with AngII positive mice scanned again two weeks post-surgery. Two weeks after pump implantation, mice were euthanized (via isofluorane inhalation and cervical dislocation) and aortas were harvested for immunohistochemical staining. Two AngII positive mice died from aneurysm rupture before the last scan at day 14. Thus, only four animals were scanned 14 days after AngII pump implantation.

Study 2 – Atherosclerosis model. Genetic alteration with and without high fat (western) diet was used to manipulate disease development in 20 male mice, in order to achieve the required varying degrees of disease burden. All mice were on a C57Bl6 mixed background (generation N7). From 6-weeks of age, mice either continued to receive regular chow or were instead fed high-fat diet (western diet). Of the mice receiving normal chow diet, 3 were wild type and 10 were genetically altered (5 Ldlr$^{-/-}$ and 5 Ldlr$^{-/-}$; GeneX$^{-/-}$). Of those receiving high fat diet, 2 were wild type and 10 were genetically altered (5 Ldlr$^{-/-}$ and 5 Ldlr$^{-/-}$;GeneX$^{-/-}$). After 12 weeks on either diet, the abdominal aorta of each mouse was scanned once using

preclinical ultrasound (refer to section 2.3 below). The average weight of mice on chow and western diet was 27.2g ± 2.09 and 31.9g ± 2.61 respectively. At the end of the study, mice were euthanized and aortas were harvested for post mortem histological assessment of atherosclerosis burden.

Ultrasound Imaging

The abdominal aorta was imaged *in-vivo* using a preclinical ultrasound system (Vevo 2100 scanner, VisualSonics, Toronto, ON, Canada) equipped with a MicroScan MS400 transducer (18 to 38MHz). Prior to imaging, anaesthetised mice were positioned supine on a heated imaging stage and hair was removed from the abdomen using hair clippers and depilatory cream. Sterile eye lubricant was applied to each eye and pre-warmed transmission gel was placed on the shaved area before scanning. Heart rate and respiration rate were noninvasively monitored through paw electrodes situated on the imaging stage. Heart rate was maintained within the range of 430–480 bpm. Body temperature was continuously monitored using a rectal temperature probe. Long-axis scans of the abdominal aorta were recorded from below the diaphragm in the suprarenal region. To avoid user-related movement, the transducer was controlled by a micrometer stage and fixed in place using a dedicated transducer mount. Careful attention was paid to image settings (gain, width and depth) in order to optimize image quality. B-mode cine loops (100-300 frames) were acquired and stored in DICOM file format for offline analysis.

Ultrasound data analysis: Manual diameter measurement

Aortic diameter measurements were performed using the accompanying Vevo2100 software (version 1.6.0). Blinded to experimental groups, manual diameter measurements were made in the same location for all samples (Figure S1a). The method involved placing a cursor on B-mode long axis ultrasound images to measure the distance between the proximal and distal wall of the abdominal aorta with respect to the transducer. Three diameter measurements were taken at peak systole and diastole, across four cardiac cycles. Arterial distension was calculated from the percent change in average lumen diameter from peak systole to peak diastole.

Ultrasound data analysis: Semi-automatic measurement

Semi-automatic analysis was carried out in Matlab (Version 2015a, MathWorks, Natick, Massachusetts, USA) using an image processing algorithm based on a probabilistic approach to track and measure the diameter of the arterial lumen over entire B-mode cine loops, as previously described by Kanber and Ramnarine. [31] Briefly, by setting the algorithm threshold to 3% and adding seed points inside the arterial lumen, the probabilistic algorithm produced arterial boundaries that were automatically tracked throughout B-mode image recordings (supplementary video). Values were averaged over a vessel region of interest (Figure S1b). Tracking of the aortic lumen diameter over the vessel region of interest (Figure S1b) produced arterial distension waveforms (Figure S2) which were used to obtain values for the lumen diameter at peak systole and peak diastole. Percent distension

was calculated as for the manual method; percent change in lumen diameter from peak systole to peak diastole. All analysis was performed by an experienced operator (J Janus), blinded to the experimental groupings.

Statistical analysis

Statistical data analysis of both studies was performed in GraphPad Prism (Version 6, Prism, California, USA). For the AAA study, study 1, comparison between two time points was made using an unpaired t-test (sham mice) or one-way ANOVA with Tukey post-hoc for three time points (AngII mice). For the atherosclerosis study, study 2, we used an unpaired t-test to examine how chow and western diet effect abdominal aorta distension. A one-way ANOVA with Tukey`s post-hoc was used to analyse data with respect to the mouse genotype and their diet. Data are represented as mean ±SEM with *$P<0.05$, **$P<0.01$ and ***$P<0.001$ considered as statistically significant.

Post-mortem analysis

Study 1 – AAA model. Changes induced by abdominal aortic aneurysm were assessed through histological and immunohistochemical examination. Mouse abdominal aortas were harvested, cleaned under dissection microscope and fixed with 10% formalin. Sections were prepared and stained with hematoxylin and eosin (H&E)[32] to identify structural changes and Elastica van Gieson (EVG) to identify elastic fibres in the aorta tissue. Other formalin fixed paraffin embedded aortic

sections were immunohistochemically stained to mark degenerative changes in smooth muscle actin (α-SMA).

Study 2 – Atherosclerosis model. For evaluation of atherosclerotic lesions, aortas were collected from the base of the ascending aorta to the level of diaphragm fixed in 4% paraformaldehyde at 4°C for 24 hours and transferred to phosphate buffered saline (PBS). After removing adventitia, aortas were opened longitudinally and stained with Oil Red O (ORO) for en face lesion analysis.[33] Positively stained arterial lesions were measured using Leica Analysis Software and expressed as a percentage of plaque coverage relative to the total surface of aorta.

Results

Study 1 – AAA model. Manual diameter measurements of the abdominal aorta revealed no change in aortic distension of mice that were scanned before and seven days after sham surgery (Figure 1a). These findings agreed with the results obtained using the semi-automatic analysis method (Figure 1b). Implantation of osmotic minipumps containing AngII produced aortic distension changes for each time point. Mice developing AAA showed disease progression seven and fourteen days after minipump implantation. Aortic distension was significantly reduced between day 0 and day 14 when analysed manually ($p<0.05$) (Figure 2a). Semi-automatic analysis of these animals showed a similar trend but with a significant difference between day 0 and day 7 ($p<0.01$) and between day 0 and day 14 ($p<0.001$) (Figure 2b).

Additionally, aneurysm development was confirmed postmortem. H&E staining revealed thickening of the adventitial layer resulting in increased total wall thickness throughout the entire circumference. Elastic Van Gieson (EVG) staining showed damage to the medial layer with visible fragmentation and disruption of the elastic lamina. In the immunochemical staining (α-SMA) samples, lost tight alignment of the elastic lamina and disorganisation of smooth muscle cell layers were observed (Figure 3).

Study 2 – Atherosclerosis model. The results showed that percent distension is highest for wild type animals on both chow and western diet than for genetically altered mice mice (Ldlr$^{-/-}$ and Ldlr$^{-/-}$;GeneX$^{-/-}$ groups). Differences between groups were not significant for the manual analysis method (Figure 4a). The semi-automatic analysis method indicated that wild type mice ($^{++/++}$) fed with chow diet had highest aortic distension with the Ldlr$^{-/-}$ group fed western diet having the lowest. The difference between these two groups was significant ($p<0.05$). A similar difference was also noted for Ldlr-/- mice with respect to diet ($p<0.05$) (Figure 4b). The effect of high fat western diet on abdominal aortic distension was assessed by grouping mice according to diet. Both the manual and semi-automatic methods showed a similar trend (Figure 5) towards decreased percent distension in the western diet group. However, only the semi-automatic method detected a significant difference between the two diets (Figure 5b). The disease state of animals has been confirmed ex-vivo by en face Oil Red O staining analysis of aortic roots. It showed high plaque distribution in mice that were fed western diet (Figure

6) with minimal plaque accumulation in mice fed chow diet. The wild type mice had the least atherosclerotic plaques distribution. Groups Ldlr$^{-/-}$ (++/--) and Ldlr$^{-/-}$; GeneX$^{-/-}$ (--/--) fed western high fat diet had the most advanced disease burden. These results were as expected and in agreement previously published data. [34-36] Further, quantitative analysis of the lesion area demonstrated that progression of atherosclerosis is linked with diet causing significant disease-related changes within aortic lumen (p<0.01).

Data variability and sample size

Generally, reduced standard deviations and coefficients of variation (CV) in percent distension were observed when applying the semi-automatic analysis method as opposed to the manual method (Table S1), indicating greater reproducibility of the semi-automatic method and the potential to detect disease-related effects using smaller group sizes. In order to quantify this effect, a retrospective power analysis was performed using distension results from both the manual and semi-automatic methods (Table 1). Here, only data from the AAA study was analyzed as the study provided percent abdominal aorta distension for both sham and diseased animals that were scanned at multiple time points. The power analysis was predicted using a significance level of 0.05, a power of 0.9 (AngII mice) or power of 0.8 (Sham mice), and prediction of a 30% difference between time points. The power analysis revealed that ten animals are required to see a 30% difference in disease progression between day 0 and day 7 when using the manual analysis method

whereas only four animals are required when using the semi-automatic method. Similarly, to detect a 30% difference between day 7 and 14, twenty four mice are needed when using the manual method whereas fifteen mice are required if data is analysed using the semi-automatic method (Table 1).

Discussion

This work investigated the feasibility of a novel semi-automatic method for tracking vessel lumen diameter changes on B-mode ultrasound images in two mouse models of vascular disease. The method uses a probabilistic approach for segmentation of ultrasound images and is based on an algorithm that was shown to have good arterial wall tracking performance comparable to that of tissue Doppler imaging. [31, 37] The efficacy of the method was originally evaluated on clinical images of the carotid arteries and the abdominal aorta.[31] The current work confirms the method can also be applied to analysis of arterial distension in preclinical studies of disease. Quantitative analysis of preclinical ultrasound data from two mouse models of vascular disease revealed that decreased percent distension is linked with disease progression in the abdominal aorta. Both analysis methods, manual and semi-automatic, show that percent distension is inversely correlated with progression of aneurysm and atherosclerotic plaque formation. These changes were significant for AngII mice that were scanned at day 0 and 7, and day 0 and 14 in study 1 (Figure 2b); and between wild-type and atherosclerosis-prone mice fed with chow or fatty diet in study 2 (Figure 4b), and were in agreement with post mortem histological analysis.

In addition to quantification of percent distension, arterial distension waveforms produced by the semi-automatic method revealed characteristic features of vessel wall motion that can be used to assess arterial health status. It was noted that reduced peak-to-trough values and broader peaks of the waveform are associated with decreased elasticity of the aorta and consequently, reduced percent distension (Figure S2). Furthermore, the dicrotic notch, associated with aortic valve closure, was clearly evident in the waveforms of healthy mice (Figure S2a) but was absent from the waveforms of diseased mice (Figure S2b).

Previous research on humans and animals indicated that arterial elasticity is linked to the structural arrangements of the artery[38] relating to cardiovascular disease and aging.[38,39] Preclinical studies showed that arterial elasticity decreases during fatty streak formation, before pathophysiological changes.[38] Leone et al concluded that carotid artery distension is an independent predictive marker of coronary heart disease in the elderly and found that carotid artery distension was associated with carotid plaque burden.[40] By combining the arterial distension results with post-mortem histological analysis (Figure 3, Figure 6) we can conclude that percent distension is inversely related to onset of AAA with associated changes in vessel wall elasticity (study 1), and increasing plaque burden (study 2). Arterial distension can therefore act as a functional early marker of vascular disease in animal models, enabling longitudinal monitoring of disease progression and response to therapeutic interventions.

Additionally, it was noted that the semi-automatic technique gives, in general, lower variance of mean percent distension than when data is analysed manually

(Figure 1,2,4,5, Table S1). The semi-automatic method may therefore be more sensitive to early signs of disease progression. Importantly, in the context of animal studies and the '3Rs' (Replacement, Reduction, Refinement), this can lead to use of fewer mice in future studies. By performing a retrospective power calculation based on the respective variances of the semi-automatic and manual analysis methods, we calculated up to a 60% reduction in the number of mice used to detect a 30% change in percent distension (Table 1). This is in addition to the reduction in number of animals used due to the fact that disease progression can be studied longitudinally in the same animals rather than requiring post-mortem analysis at each time point.

The semi-automatic analysis method and the quality of the resultant distension waveforms is strongly dependent on image quality and tissue motion in all directions. It is important to obtain B-mode recordings with high image contrast i.e. low-intensity lumen signal and high-intensity vessel wall signal, to enable reliable vessel wall tracking. Here, features of the abdominal aorta such as length, straightness, minimal aortic motion out of plane and ease in locating, made the abdominal aorta the ideal vessel to investigate the performance of this semi-automatic method for ultrasound data analysis. The semi-automatic method, unlike the manual method, has the advantage of averaging mechanical changes over a larger vessel region of interest rather than relying on manual, single point measurements of the vessel lumen in the systolic and diastolic phase. This makes the semi-automatic method less user-dependent, less variable and consequently more sensitive to real changes in arterial distension.

We believe that this work represents an important development for future preclinical studies of vascular disease. The semi-automatic analysis method results in reduced user-dependency, reduced data variability (and consequently reduced sample sizes) and increased sensitivity of preclinical ultrasound to early signs of disease progression. Future studies will focus on additional vascular disease models and the evaluation of therapeutic strategies aimed at reducing the deterioration in arterial distension observed in these studies.

References

1.   Carovac A, Smajlovic F and Junuzovic D. Application of ultrasound in medicine. *Acta Inform Med*. 2011; 19: 168-71.
2.   Steinl DC and Kaufmann BA. Ultrasound imaging for risk assessment in atherosclerosis. *Int J Mol Sci*. 2015; 16: 9749-69.
3.   Scaife M, Giannakopoulos T, Al-Khoury GE, Chaer RA and Avgerinos ED. Contemporary Applications of Ultrasound in Abdominal Aortic Aneurysm Management. *Front Surg*. 2016; 3: 29.
4.   Dua MM and Dalman RL. Hemodynamic influences on abdominal aortic aneurysm disease: Application of biomechanics to aneurysm pathophysiology. *Vascul Pharmacol*. 2010; 53: 11-21.
5.   Xu J and Shi GP. Vascular wall extracellular matrix proteins and vascular diseases. *Biochim Biophys Acta*. 2014; 1842: 2106-19.
6.   Yang WI and Ha JW. Non-invasive assessment of vascular alteration using ultrasound. *Clin Hypertens*. 2015; 21: 25.
7.   Kaufmann BA. Ultrasound molecular imaging of atherosclerosis. *Cardiovascular research*. 2009; 83: 617-25.

8.   Crouse JR, Furberg CD, Espeland MA and Riley WA. B-mode ultrasound: a noninvasive method for ssessing atherosclerosis. *CARDIOVASC MED*. 2007: 1783-96.

9.   Silverstein MD, Pitts SR, Chaikof EL and Ballard DJ. Abdominal aortic aneurysm (AAA): cost-effectiveness of screening, surveillance of intermediate-sized AAA, and management of symptomatic AAA. *Proc (Bayl Univ Med Cent)*. 2005; 18: 345-67.

10.   Goel S, Miller A, Agarwal C, et al. Imaging Modalities to Identity Inflammation in an Atherosclerotic Plaque. *Radiol Res Pract*. 2015; 2015: 410967.

11.   Patel AK, Suri HS, Singh J, et al. A Review on Atherosclerotic Biology, Wall Stiffness, Physics of Elasticity, and Its Ultrasound-Based Measurement. *Curr Atheroscler Rep*. 2016; 18: 83.

12.   Baltgaile G. Arterial wall dynamics. *Perspectives in Medicine* 2012; 1: 146-51.

13.   Godia EC, Madhok R, Pittman J, et al. Carotid artery distensibility: a reliability study. *Journal of ultrasound in medicine : official journal of the American Institute of Ultrasound in Medicine*. 2007; 26: 1157-65.

14.   De Souza R, Spence T, Huang H and Allen C. Preclinical imaging and translational animal models of cancer for accelerated clinical implementation of nanotechnologies and macromolecular agents. *J Control Release*. 2015; 219: 313-30.

15.   Du W, Tao H, Zhao S, He ZX and Li Z. Translational applications of molecular imaging in cardiovascular disease and stem cell therapy. *Biochimie*. 2015; 116: 43-51.

16.   Peshkova IO, Schaefer G and Koltsova EK. Atherosclerosis and aortic aneurysm - is inflammation a common denominator? *FEBS J*. 2016; 283: 1636-52.

17.   Daugherty A and Cassis LA. Mouse models of abdominal aortic aneurysms. *Arterioscler Thromb Vasc Biol*. 2004; 24: 429-34.

18.   Favreau JT, Nguyen BT, Gao I, et al. Murine ultrasound imaging for circumferential strain analyses in the angiotensin II abdominal aortic aneurysm model. *J Vasc Surg*. 2012; 56: 462-9.

19.   Zadelaar S, Kleemann R, Verschuren L, et al. Mouse models for atherosclerosis and pharmaceutical modifiers. *Arterioscler Thromb Vasc Biol*. 2007; 27: 1706-21.

20.   Goergen CJ, Barr KN, Huynh DT, et al. In vivo quantification of murine aortic cyclic strain, motion, and curvature: implications for abdominal aortic aneurysm growth. *J Magn Reson Imaging*. 2010; 32: 847-58.

21.   Whitman SC. A practical approach to using mice in atherosclerosis research. *Clin Biochem Rev*. 2004; 25: 81-93.

22.   Barisione C, Charnigo R, Howatt DA, Moorleghen JJ, Rateri DL and Daugherty A. Rapid dilation of the abdominal aorta during infusion of angiotensin II detected by noninvasive high-frequency ultrasonography. *J Vasc Surg*. 2006; 44: 372-6.

23.   Azuma J, Maegdefessel L, Kitagawa T, Dalman RL, McConnell MV and Tsao PS. Assessment of elastase-induced murine abdominal aortic aneurysms:

comparison of ultrasound imaging with in situ video microscopy. *J Biomed Biotechnol*. 2011; 2011: 252141.

24.	Cao RY, Amand T, Ford MD, Piomelli U and Funk CD. The Murine Angiotensin II-Induced Abdominal Aortic Aneurysm Model: Rupture Risk and Inflammatory Progression Patterns. *Front Pharmacol*. 2010; 1: 9.

25.	Martin-McNulty B, Vincelette J, Vergona R, Sullivan ME and Wang YX. Noninvasive measurement of abdominal aortic aneurysms in intact mice by a high-frequency ultrasound imaging system. *Ultrasound Med Biol*. 2005; 31: 745-9.

26.	Zhang X, Ha S, Wei W, Duan S, Shi Y and Yang Y. Noninvasive imaging of aortic atherosclerosis by ultrasound biomicroscopy in a mouse model. *Journal of ultrasound in medicine : official journal of the American Institute of Ultrasound in Medicine*. 2015; 34: 111-6.

27.	Li RJ, Sun Y, Wang Q, et al. Ultrasound Biomicroscopic Imaging for Interleukin-1 Receptor Antagonist-Inhibiting Atherosclerosis and Markers of Inflammation in Atherosclerotic Development in Apolipoprotein-E Knockout Mice. *Tex Heart Inst J*. 2015; 42: 319-26.

28.	Dall'Ara E, Boudiffa M, Taylor C, et al. Longitudinal imaging of the ageing mouse. *Mech Ageing Dev*. 2016; 160: 93-116.

29.	Coatney RW. Ultrasound imaging: principles and applications in rodent research. *ILAR J*. 2001; 42: 233-47.

30.	Trachet B, Fraga-Silva RA, Londono FJ, Swillens A, Stergiopulos N and Segers P. Performance comparison of ultrasound-based methods to assess aortic diameter and stiffness in normal and aneurysmal mice. *PLoS One*. 2015; 10: e0129007.

31.	Kanber B and Kumar VR. A probabilistic approach to computerized tracking of arterial walls in ultrasound image sequences. *ISRN Signal Processing*. 2012; 179087: 11.

32.	Venegas-Pino DE, Banko N, Khan MI, Shi Y and Werstuck GH. Quantitative analysis and characterization of atherosclerotic lesions in the murine aortic sinus. *J Vis Exp*. 2013: 50933.

33.	Paigen B, Morrow A, Holmes PA, Mitchell D and Williams RA. Quantitative assessment of atherosclerotic lesions in mice. *Atherosclerosis*. 1987; 68: 231-40.

34.	Emini Veseli B, Perrotta P, De Meyer GRA, et al. Animal models of atherosclerosis. *Eur J Pharmacol*. 2017; 816: 3-13.

35.	Getz GS and Reardon CA. Animal models of atherosclerosis. *Arterioscler Thromb Vasc Biol*. 2012; 32: 1104-15.

36.	Ma Y, Wang W, Zhang J, et al. Hyperlipidemia and atherosclerotic lesion development in Ldlr-deficient mice on a long-term high-fat diet. *PLoS One*. 2012; 7: e35835.

37.	Ramnarine KV, Kanber B and Panerai RB. Assessing the performance of vessel wall tracking algorithms: the importance of the test phantom. *J Phys Conf Ser*. 2004; 1: 199-204.

38.	Leeson CP, Whincup PH, Cook DG, et al. Cholesterol and arterial distensibility in the first decade of life: a population-based study. *Circulation*. 2000; 101: 1533-8.

39.   Kuo MM, Barodka V, Abraham TP, et al. Measuring ascending aortic stiffness in vivo in mice using ultrasound. *J Vis Exp*. 2014.

40.   Leone N, Ducimetiere P, Gariepy J, et al. Distension of the carotid artery and risk of coronary events: the three-city study. *Arterioscler Thromb Vasc Biol*. 2008; 28: 1392-7.
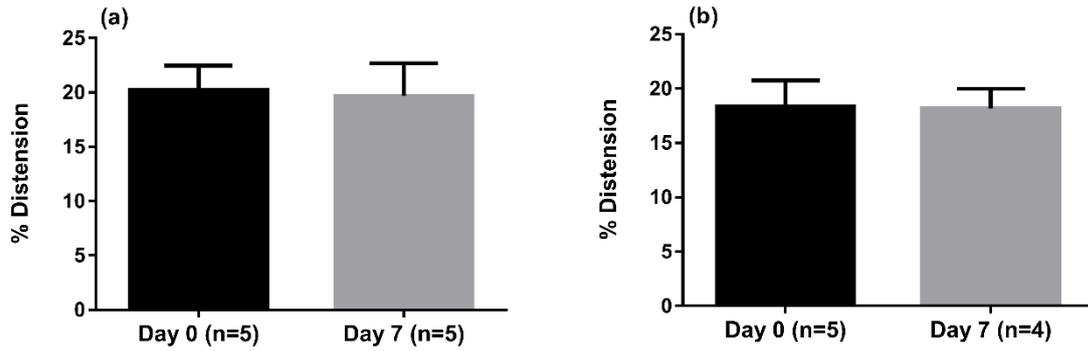
Figure 1. Percent distension of the abdominal aorta in sham control mice. Results were obtained through manual diameter measurements (a) and semi-automatic analysis (b). Bar charts represent mean ± SEM percent distension. Unpaired t-test showed no significant difference for both methods (p<0.05).
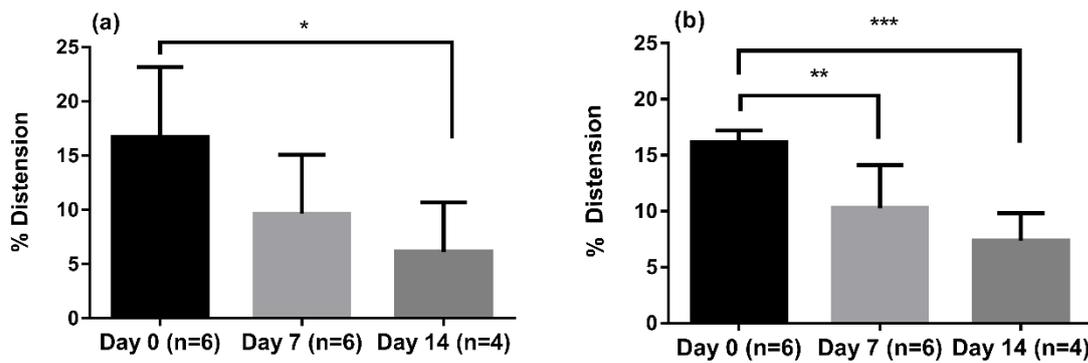

Figure 2. Percent distension of the abdominal aorta in Angiotensin II mice. Results were obtained through manual diameter measurements (a) and semi-automatic analysis (b). Bar charts represent mean ± SEM percent distension. One way ANOVA with Tukey post-hoc test revealed significantly reduced distension at day 14 compared to baseline in (a) and at both day 7 and day 14 compared to baseline in (b) (p<0.05).
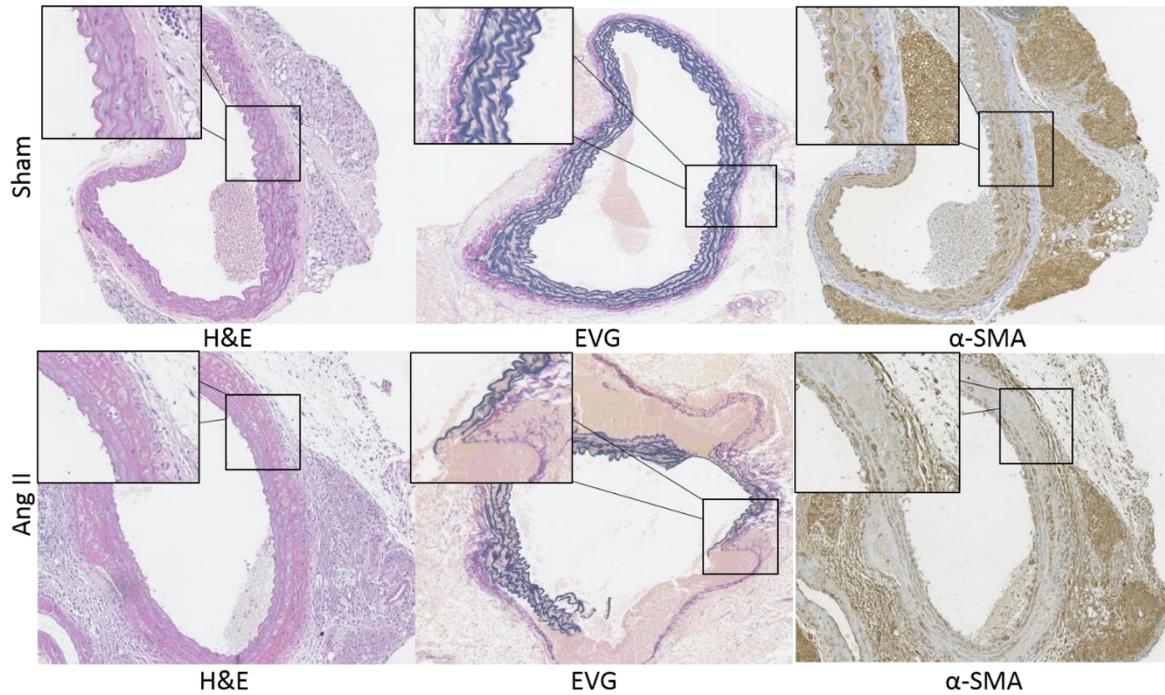
Figure 3. Representative images of abdominal aorta cross-sections after histological staining with Hematoxylin Eosin (H&E), Elastic van Gieson (EVG) and Immunochemical staining for Anti-alpha smooth muscle Actin (α-SMA) in sham and angiotensin II (AngII) positive mice. H&E staining revealed thickening of the adventitial layer, EVG staining showed damage to the medial layer with fragmentation of the elastic lamina and α-SMA samples revealed loss of tight alignment of the elastic lamina and disorganisation of smooth muscle cell layers in AngII mice.
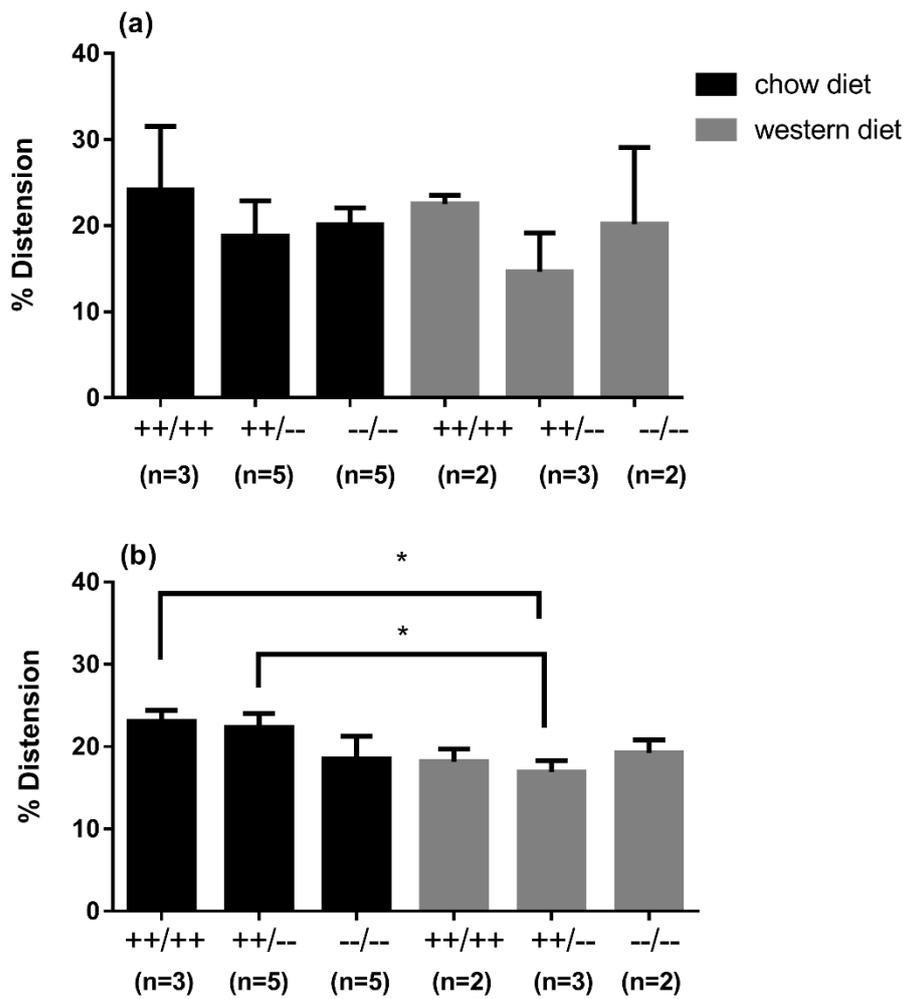
Figure 4. Percent distension of the abdominal aorta for mice in the atherosclerosis study (study 2) obtained through manual diameter measurements (a) and semi-automatic analysis (b). Animals were grouped and compared according to genotype and diet. Bar charts represents mean ± SEM percent distension. Significance was tested using one way ANOVA with Tukey post-hoc test (p<0.05). Genotypes: wild type (++/++), Ldlr$^{-/-}$ (++/--), Ldlr$^{-/-}$; GeneX$^{-/-}$ (--/--).
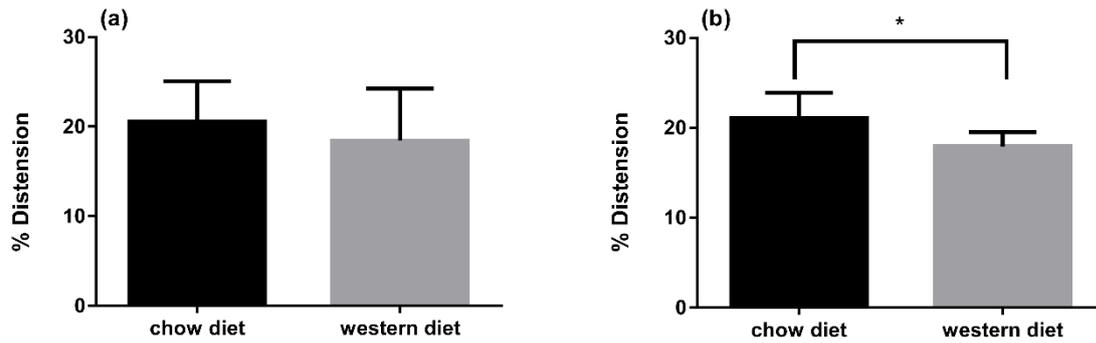
Figure 5. Percent distension of the abdominal aorta for mice in the atherosclerosis study (study 2) obtained through manual diameter measurements (a) and semi-automatic analysis (b) in mice fed chow (n=13) vs western diet (n=7). Bar charts represents mean ± SEM percent distension. The analysis shows a significant difference between groups when data was analysed using the semi-automatic method. Significance was tested using an unpaired Student`s t-test (p<0.05).
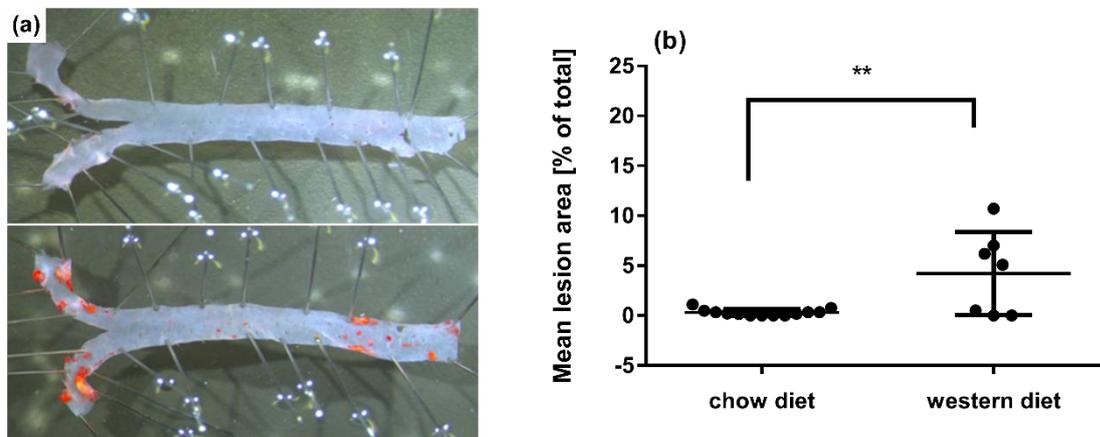

Figure 6. (a) Representative *en face* Oil Red O (ORO) staining showing atherosclerotic plaque distribution in the aortic root of mice fed chow diet (top) and western diet (bottom) in study 2. Quantitative analysis of the lesion area in mice aortic roots revealed a significant difference between chow (n=13) and western (n=7) diet (b). The positively stained arterial lesions area was measured and expressed as a percent of plaque coverage, relative to the total surface of aorta. Data shown as mean ± SD. Significance was tested using an unpaired Student`s t-test (p<0.05)

	day 0 vs day 7		day 7 vs day 14	
Method	Manual	Semi-automatic	Manual	Semi-automatic
Power	0.9		0.9	
Significance level	0.05		0.05	
Anticipated diffrence	30%		30%	
Predicted group size	**10**	**4**	**24**	**15**

Table 1. Power analysis of required animal group size in AAA study for detecting significant difference between time points when using the manual and semi-automatic analysis methods. The difference between the two methods was determined using a power of 0.9, a significance level of 0.05 and predicted 30% difference in aneurysm development between two time points.
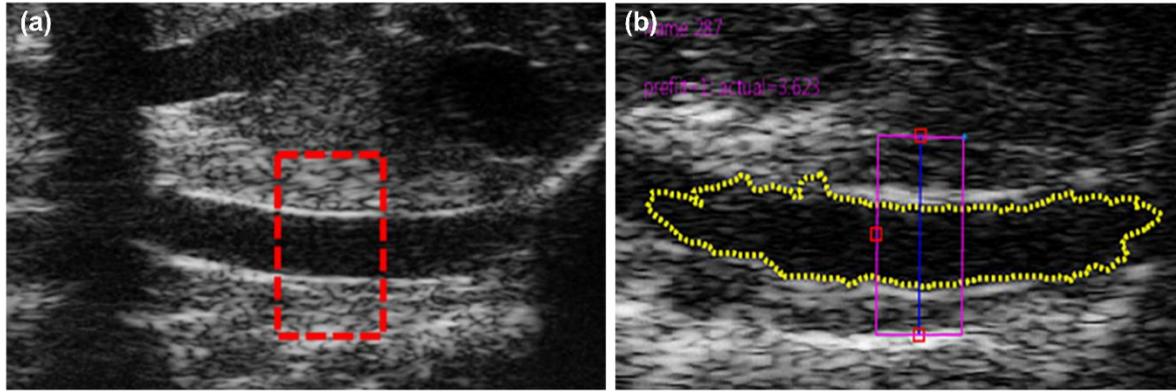
Figure S1. Longitudinal view of abdominal aorta with illustration of manual diameter measurement area (a) and representative image of tracking and measuring lumen diameter using the semi-automatic method (b). Manual measurements in (a) were taken approximately 2-3 mm below the diaphragm within 2-3 mm window (red). Image (b) shows semi-automatic tracking of vessel walls (yellow) and the segment of vessel used for lumen diameter measurements (purple rectangle).
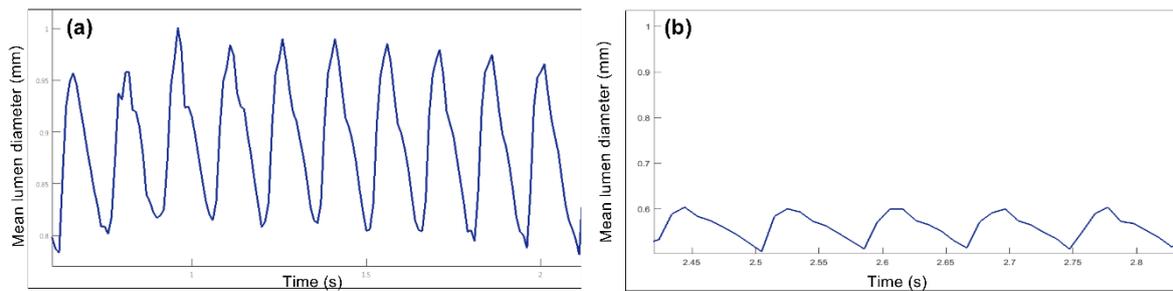

Figure S2. Example of arterial distension waveforms from (a) healthy mouse with 0.92 mm arterial lumen diameter and (b) atherosclerotic mouse with 0.69 mm lumen diameter (means of means) over multiple cardiac cycles measured by the semi-automatic method. Reduced average peak-to-trough values in the atherosclerotic mouse indicate a reduction in arterial distension.

Study 1 - AAA model	Manual method				Semi- automatic method			
Mouse group	N	Mean	St.dev	CV	N	Mean	St.dev	CV
Sham- day 0	5	20.26	2.205	10.88%	5	18.34	2.421	13.20%
Sham- day 7	5	19.68	2.991	15.20%	4	18.17	1.807	9.94%
AngII -day 0	6	16.75	6.434	38.42%	6	16.1	1.05	6.48%
AngII -day 7	6	9.628	5.442	56.53%	6	10.3	3.85	37.49%
AngII -day 14	4	6.134	4.558	74.31%	4	7.36	2.48	33.73%

Study 2 - Atherosclerosis model	Manual method				Semi-automatic method			
Mouse group	N	Mean	St.dev	CV	N	Mean	St.dev	CV
chow diet								
Wild type (++/++)	3	24.12	7.413	30.73%	3	23.07	1.327	5.75%
Ldlr-/- (++/--)	5	18.79	4.08	21.72%	5	22.37	1.646	7.36%
Ldlr-/-; GeneX-/- (--/--)	5	20.12	1.941	9.65%	5	18.47	2.792	15.12%
western diet								
Wild type (++/++)	2	22.49	1.025	4.56%	2	18.16	1.549	8.53%
Ldlr-/- (++/--)	3	14.64	4.513	30.83%	3	16.94	1.38	8.15%
Ldlr-/-; GeneX-/- (--/--)	2	20.16	8.895	44.12%	2	19.22	1.598	8.31%

Table S1. Mean, standard deviation and coefficient of variation of % distension for mice in both studies obtained using the manual and semi-automatic analysis methods.

Supplementary video. B-mode image recording of abdominal aorta used in combination with a semi-automatic image processing method to track arterial distension alterations in AAA and atherosclerosis mouse models (Codec used: H264).